Islamic Azad University

Journal of
Optoelectronical Nanostructures

Winter 2020 / Vol. 5, No. 1

Numerical Modeling of a Metamaterial Biosensor for Cancer Tissues Detection

Hamed Emami Nejad[1], Ali Mir[1], Ali Farmani[*,1]

[1] Faculty of Engineering, Lorestan University, KhoramAbad, Iran

(Received 10 Dec. 2019; Revised 23 Jan. 2020; Accepted 21 Feb. 2020; Published 15 Mar. 2020)

Abstract: In this paper, the numerical design and simulate a biosensor to detect tumors and cancerous tissues by using metamaterial structures in the microwave regime are presented. The presented structure consists of a microstrip transmission line and a split ring resonator (SRR) that form a bandpass filter and has a unique resonance frequency. Given that cancerous tissues have larger volumes of water than healthy tissues. As a result, they have a higher dielectric coefficient and conductivity which use for healthy tissues detection. By placing biological samples on SRR, its dielectric constant changes, therefore, the resonance frequency of the system changes. We can measure the types of biological tissues by measuring these changes. We used the Debye model to simulate the muscles. Also, the benefits of this biosensor are easy to use and operation, but they have lower sensitivity than terahertz biosensors. The minimum resolution for samples under test in this biosensor is 10 MHz.

Keywords: Biosensor, Microstrip Line, Split Ring Resonator, Cancerous Tissues, Debye Model.

1. INTRODUCTION

More recently, the metamaterials have been considered by several research groups due to their interesting optical properties including negative the dielectric constant (ε) and the magnetic permeability (μ) [1], as well as their application such as microsphere sensor [1], second harmonic generation [2], plasmonics sensor [3-7], biosensors [8-12], refractive and optical sensors [13-30], and etc [31-41]. One of the most critical features of this material is the negative refractive index as well as the guidance of electromagnetic waves in the desired direction [42-56]. It is worth mentioning that two dimensional material have been received much attention from research groups [57-58]. Considering the extremely high sensitivity of metamaterials to electromagnetic waves, they are also used as biological sensors. Conventional biological sensors

* Corresponding author. Email: **Farmani.a@lu.ac.ir**

(such as those works based on electromechanical transfer, fluorescence, nanomaterials and surface plasma resonance) often suffer from their very sophisticated equipment. In recent years, researchers have proposed the use of metamaterials for high sensitive to chemicals, biochemistry, and biological analytes. However, many of these structures suffer from their complicated fabrication and their cost.

In this paper, we design and simulate a low-cost and straightforward biosensor in the microwave ranges. The proposed sensor is made up of a macro strip line and a split ring resonator (SRR). The SRR can be considered as a simple LC circuit, which has a specific resonance frequency, which depends on the dimensions and the dielectric constant (ε). We also know that cancerous tissues and tumors have a higher content of water than healthy tissues. Hence, they have higher dielectric constant as well as conductivity. As a result, we can use these changes to detect these tissues from each other. By placing the tissues on the SRRs, the dielectric constant of the medium changes and the resonant frequency is then shifted. By measuring the rate of the shift, one can recognize the tissues and their types. Because the dielectric constant and the conductivity of biological tissues vary with frequency, we have used the Debye model to account for these effects.

2. THE MODEL OF THE PROPOSED BIOSENSOR

The three-dimensional schematic of the proposed biosensor structure is shown in Fig. 1. As can be seen, this sensor is composed of a microstrip line and an SRR. Electric waves are emitted from the input port and measured at the output port. SR can be considered equivalent to a simple LC circuit.

Fig. 2 shows an example of SRR whose resonant frequency is obtained by equation 1-2.

$$c = \varepsilon_0 \varepsilon_c \frac{d}{a}, L = \mu_0 \frac{w^2}{d_1} \tag{1}$$

$$\omega_{LC} = \frac{1}{\sqrt{LC}} = \frac{1}{w}\frac{c}{\sqrt{\varepsilon_c}}, c = \frac{1}{\sqrt{\varepsilon_0 \mu_0}} \tag{2}$$

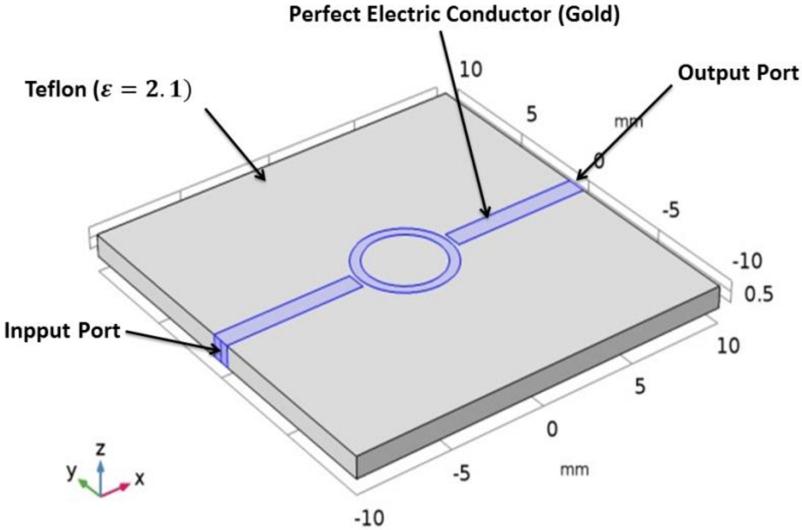

Fig. 1 The overall shape of the proposed biosensor

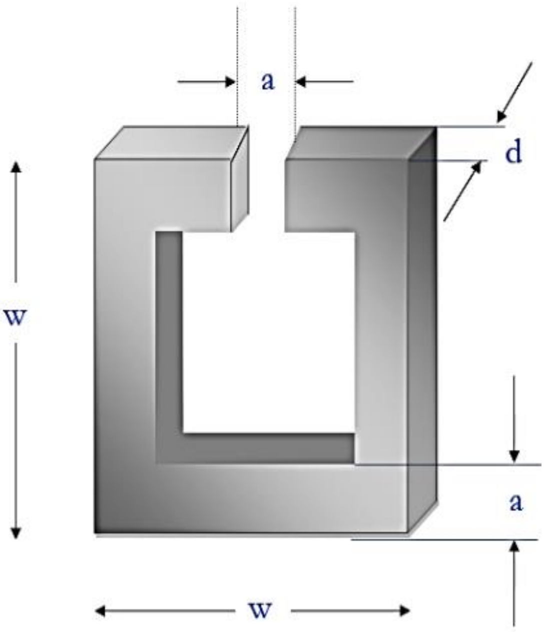

Fig. 2 An example of SRR

In the Fig. 3, the exact dimensions of sensor are considered that are L=7.3 mm, h=1 mm, g=0.2 mm, R1=2 mm, and R2=2.5 mm.

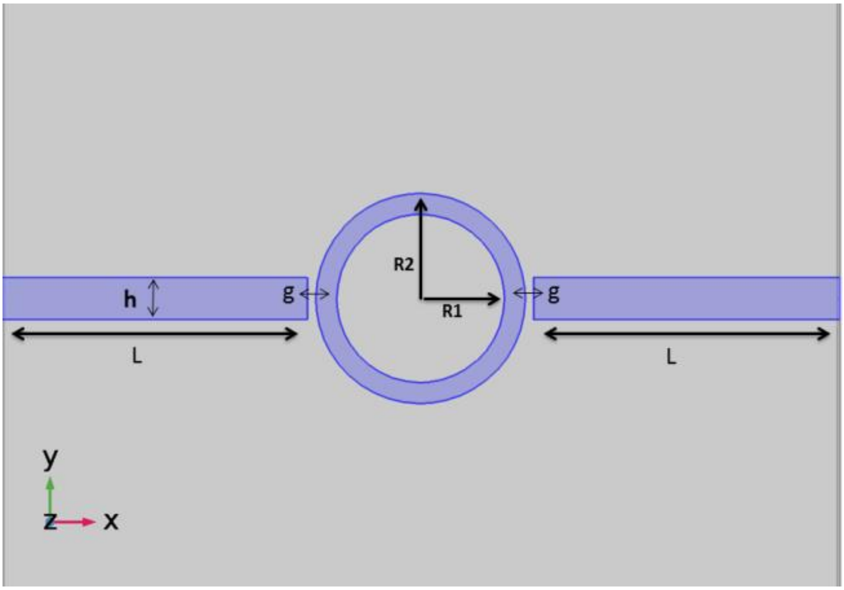

Fig. 3 Dimensions of the sensor

3. REQUIRED INFORMATION FOR SIMULATION

As mentioned in the earlier section, in this work, the Debye model is utilized; hence, in this section examines the essential information for simulation [59,60]. As we have mentioned, for the detection of tissues from each other, we use here the constant dielectric and conductivity changes in normal and malignant tissues. For modeling of biological tissues and simulate them, we use the Debye model whose relations are shown in Equations 3-5.

$$\varepsilon_{rc}(\omega) = \varepsilon_r(\omega) + i\frac{\sigma(\omega)}{\omega\varepsilon_0} \tag{3}$$

$$\varepsilon_r(\omega) = \varepsilon_\infty(\omega) + \frac{\varepsilon_s}{1+(\omega\tau)^2} \tag{4}$$

$$\sigma(\omega) = \omega^2\tau\varepsilon_0\frac{\varepsilon_s - \varepsilon_\infty}{1+(\omega\tau)^2} + \sigma_s \tag{5}$$

The parameters extracted from the tissues of the body outside for healthy, cirrhotic, malignant, and tumor specimens are shown in the following table [61].

Table I. the parameters of *ex vivo*

Materials	τ [ps]	ε_{∞}	ε_{s}	σ_{s}
Normal	11.55	5.32	49.55	0.25
Malignant	10.82	4.60	58.86	0.21
Cirrhotic	10.45	6.09	52.9	0.74
Tumor	15	18.8	46.8	0.803

The Fig. 4 illustrates the results of simulation of Debye model for relative permittivity (top charts) and effective conductivity (bottom charts) as a function of frequency for all the tissues including of normal, malignant, cirrhotic and tumor, respectively, in the frequency range between 1 to 20 GHz.

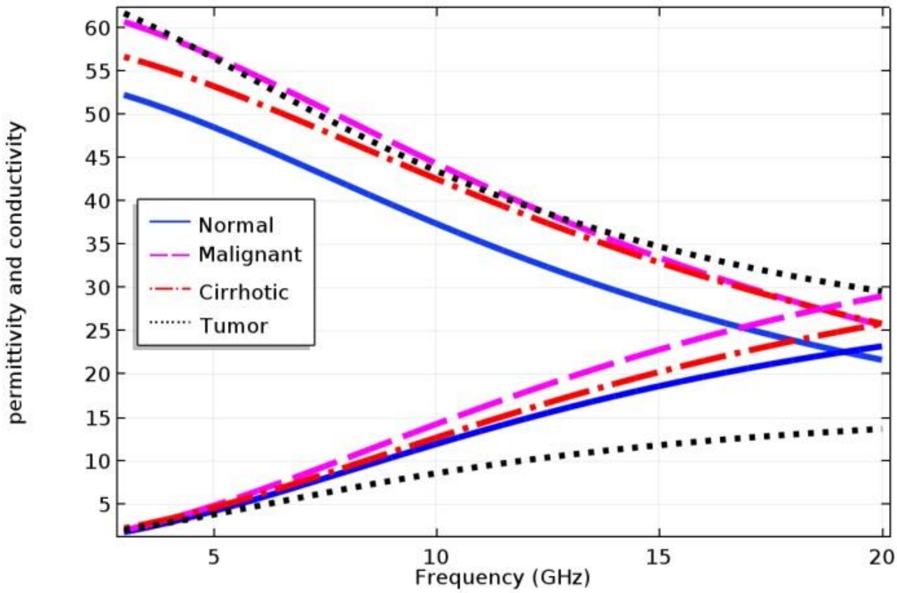

Fig. 4. Effective conductivity and relative permittivity VS frequency in the GHz regime

We used the reflection and transmission parameters to detect of tissues, which is obtained as $T=|S_{21}|^2$and $R=|S_{11}|^2$. The method used here for the process of simulating and solving differential equations is the finite element method (FEM) [62]. The FEM is an accurate numerical solution method based on meshed structures, and then equations and boundary conditions are solved in each mesh. This method is more precise than other methods and is well adapted to non-square structures. Also, the equations we want to solve using this method are the following equations:

$$\nabla \times \mu_r^{-1}(\nabla \times E) - k_0^2(\varepsilon_r - \frac{j\sigma}{\omega\varepsilon_0})E = 0 \quad (6)$$

$$E(x,y,z) = E(x,y)e^{ik_z z} \quad (7)$$

Here, E is the electric field, μ_r and ω are the relative permeability tensor and the angular frequency, respectively. The σ is the conductivity tensor, ε_0 is the permittivity of the vacuum, ε_r is the relative permittivity tensor, and finally, k_0 is the free space wave number.

4. RESULTS AND DISCUSSION

As mentioned in section 1, the proposed sensor has a SRR structure [63], and acts as a band-pass filter, which has a resonant frequency. In Fig. 6, the reflection and transmission diagrams of the sensor are shown for a case in which there is no sample on it. In this case, the resonance frequency of the system is 15.3 GHz.

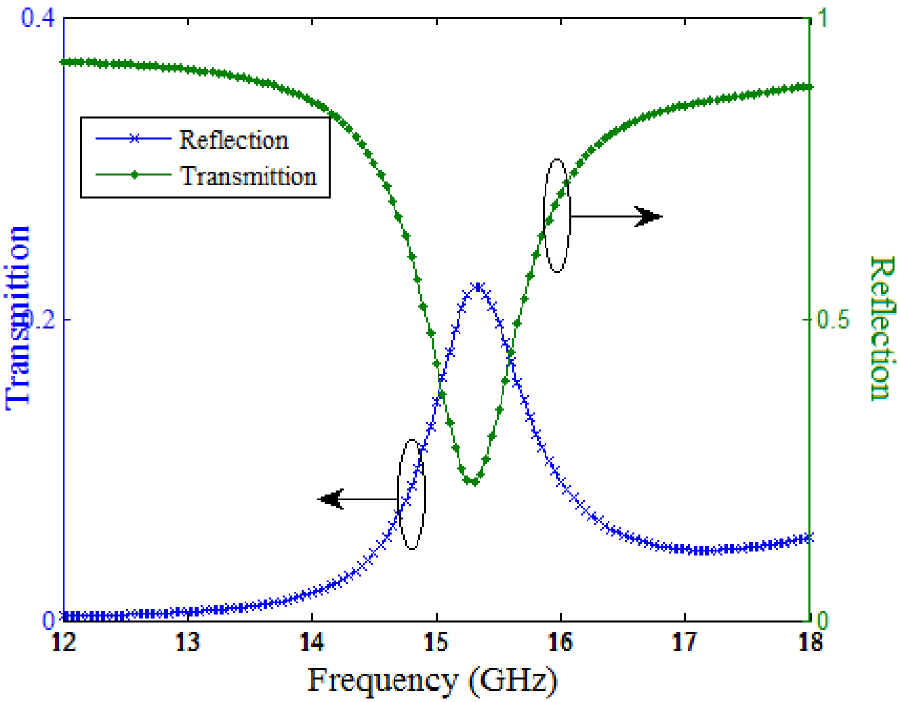

Fig. 6: The frequency response of the proposed biosensor

Also, in Fig. 7, we can see the distribution of the electric field at the resonance frequency. At this frequency, we will have the maximum transmission of electrical waves.

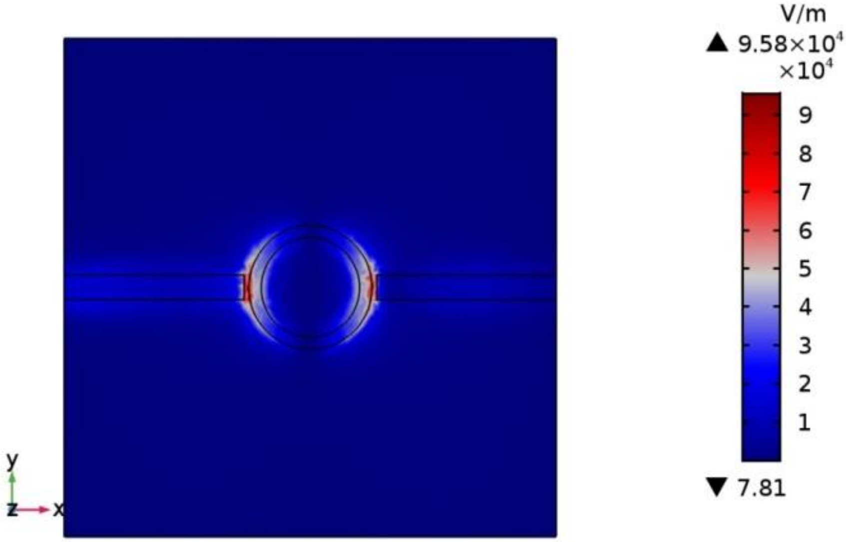

Fig. 7: Distribution of the electric field at a resonance frequency of 15.3 GHz

As mentioned in the previous section, if we put the samples, we show on the SRR, the dielectric constant of the medium is changed, and as a result, the resonant frequency of the system is shifted. In Fig. 8, these changes are shown for healthy, cirrhotic, malignant, and tumor tissues.
The changes in the resonance frequency of the system in various modes are respectively, 15.3 (no sample), 16.65 (standard sample), 16.6 (Cirrhotic), 16.59 (Malignant), and 16.7 (Tumor). As can be mentioned above, each of the tissues has a specific resonance frequency, which is due to their dielectric constant. According to the results, at least the resolution for the separation between the samples is about 10 MHz, which is related to the cirrhotic and malignant tissues. The maximum value is 110 MHz, which is related to malignant and tumor. In future the sensing behavior in our works is considered [64-66].
For future works, one-two dimensional can be considered [67-79].

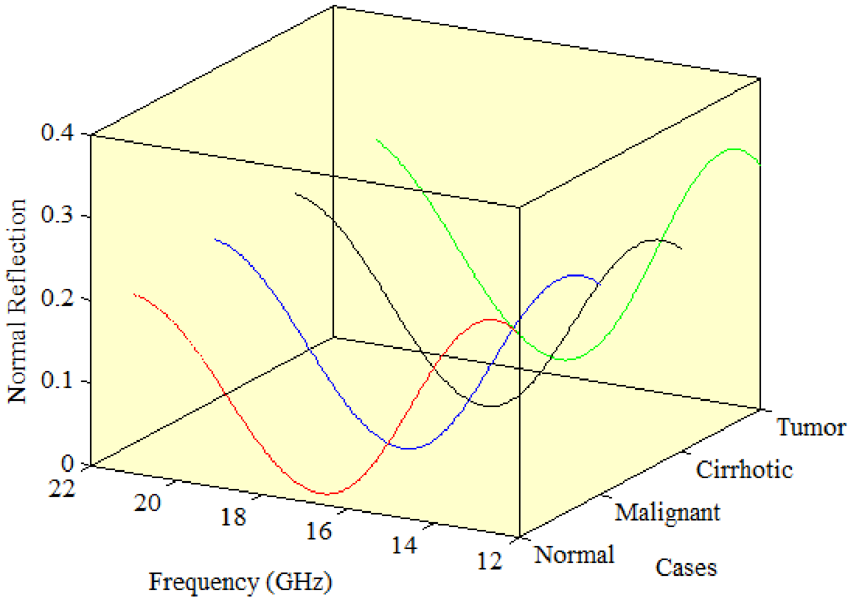

Fig. 8 The frequency response for all the tissues

5. CONCLUSION

In this paper, we simulated biosensor based on metamaterials for cancerous tissues detection in the microwave regime. Since biological tissues have certain dielectric constant and conductivity, we used this issue to identify them. In the absence of samples, the sensor has a specific resonance frequency, which, by placing the sample on it, will shift the frequency. The minimum and maximum resolution for the tested samples is 10 and 110 MHz. The advantages of this sensor include smooth operation and manufacturing.

REFERENCES

[1] Heshmati, Sajjad, Kambiz Abedi, and Ghafar Darvish. *Investigation of the Effect of Notch and Particle Geometries on Performance of WGM Microsphere Sensor*. IEEE Sensors Journal 19.1 (2019): 151-156. Available: 10.1109/JSEN.2018.2874645

[2] Hamidi, Jafar, and Mahdi Zavvari. *Strong coupling of metamaterial resonances to intersubband transitions of quantum dots for enhanced second-harmonic generation*. Applied optics 57.36 (2018): 10505-10509. Available: https://doi.org/10.1364/AO.57.010505

[3] Ahmadi, H., et al. *Evaluation of single virus detection through optical biosensor based on microsphere resonator*. Optik-International Journal for

Light and Electron Optics 125.14 (2014): 3599-3602. Available: https://doi.org/10.1016/j.ijleo.2014.01.087

[4] Golmohammadi, Saeed, Arash Ahmadivand, and Nezih Pala. *Fano Resonances in Nanoshell Clusters Deposited on a Multilayer Substrate of $\bm\beta $-SiC/SiO 2/Si to Design High-Quality Plasmonic Sensors*. Journal of Lightwave Available: 10.1109/JLT.2015.2414439

[5] Ghorbanzadeh, Mostafa, Mohammad Kazem Moravvej-Farshi, and Sara Darbari. *Plasmonic Optophoresis for Manipulating, In Situ Position Monitoring, Sensing, and 3-D Trapping of Micro/Nanoparticles*. IEEE Journal of Selected Topics in Quantum Electronics 23.2 (2017): 185-192. Technology 33.13 (2015): 2817-2823. Available: 10.1109/JSTQE.2016.2593008

[6] Emami-Nejad, Hamed, and Ali Mir. *Design and simulation of a flexible and ultra-sensitive biosensor based on frequency selective surface in the microwave range.* Optical and Quantum Electronics 49.10 (2017): 320. Available: https://doi.org/10.1007/s11082-017-1147-8

[7] Dolatabady, A., and N. Granpayeh. *Nanoscale temperature sensor based on plasmonic waveguides with nanocavity resonator*. the second Irannian Conference on Engineering Electromagnetics (ICEEM 2014). 2014. Available: isseem.ir

[8] Abbasi, Mohammad, Mohammad Soroosh, and Ehsan Namjoo. *Polarization-insensitive temperature sensor based on liquid filled photonic crystal fiber*. Optik 168 (2018): 342-347. Available: https://doi.org/10.1016/j.ijleo.2018.04.116

[9] Dolatyari, Mahboubeh, et al. *Fluorescence Resonance Energy Transfer between an Anti-EGFR Antibody and Bi2Se3/SiO2, ZnS/SiO2, and ZnSe/SiO2 Nanomaterials for Biosensor Purposes*. Zeitschrift für anorganische und allgemeine Chemie 643.21 (2017): 1564-1571. Available: https://doi.org/10.1002/zaac.201700257

[10] Fang, N., Lee, H., Sun, C., Zhang, X., *Sub-diffraction-limited optical imaging with a silver superlens*, Science 308, 534–537 (2005). Available: 10.1126/science.1108759

[11] Khozeymeh, Foroogh, and Mohammad Razaghi. *Characteristics optimization in single and dual coupled silicon-on-insulator ring (disk) photonic biosensors*. Sensors and Actuators B: Chemical 281 (2019): 998-1008. Available: https://doi.org/10.1016/j.snb.2018.11.017

[12] Mozaffari, Mohammad Hazhir, et al. *designing a miniaturized photonic crystal based optofluidic biolaser for lab-on-a-chip biosensing applications*. Organic Electronics 54 (2018): 184-191. Available: https://doi.org/10.1016/j.orgel.2017.12.040

[13] Ebnali-Heidari, Majid, et al. *Designing Tunable Miniaturized Spectroscopic Gas Sensor Using Optofluidic Hollow-Core Photonic Crystal Fiber*. Optical Sensors. Optical Society of America, 2014. Available: https://doi.org/10.1364/SENSORS.2014.SeTh4C.4

[14] Ramanujam, Nambi R., et al. *Enhanced sensitivity of cancer cell using one dimensional nano composite material coated photonic crystal*. Microsystem Technologies 25.1 (2019): 189-196. Available: https://doi.org/10.1007/s00542-018-3947-6

[15] Rakhshani, Mohammad Reza, Alireza Tavousi, and Mohammad Ali Mansouri-Birjandi. *Design of a plasmonic sensor based on a square array of nanorods and two slot cavities with a high figure of merit for glucose concentration monitoring.* Applied optics 57.27 (2018): 7798-7804. Available: https://doi.org/10.1364/AO.57.007798

[16] Karampour, Nasrollah, and Najmeh Nozhat. *Infrared-Visible Ultra-Wide Band Polarization-Independent Metamaterial Absorber Utilizing Low Conductivity π-Shaped Element*. Plasmonics (2018): 1-9. Available: https://doi.org/10.1007/s11468-018-0766-7

[17] Farmani, Ali., *Three-dimensional FDTD analysis of a nanostructured plasmonic sensor in the near-infrared range*. JOSA B 36.2 (2019): 401-407. Available: https://doi.org/10.1364/JOSAB.36.000401

[18] Baqir, M. A., et al., *Nanoscale, tunable, and highly sensitive biosensor utilizing hyperbolic metamaterials in the near-infrared range*. Applied optics 57.31 (2018): 9447-9454. Available: https://doi.org/10.1364/AO.57.009447

[19] Ghodrati, Maryam, Ali Farmani, and Ali Mir., *Nanoscale Sensor-based Tunneling Carbon Nanotube Transistor for Toxic Gases Detection: A First-Principle Study*. IEEE Sensors Journal (2019). Available: 10.1109/JSEN.2019.2916850

[20] Mansuri, Morteza, Ali Mir, and Ali Farmani., *Numerical Modeling of a Nanostructure Gas Sensor Based on Plasmonic Effect*. Journal of Optoelectronical Nanostructures 4.2 (2019): 29-44. Available: http://jopn.miau.ac.ir/article_3476_479.html

[21] Farmani, Ali, and Ali Mir., *Graphene Sensor Based on Surface Plasmon Resonance for Optical Scanning*. IEEE Photonics Technology Letters 31.8 (2019): 643-646. Available: 10.1109/LPT.2019.2904618

[22] Nejad, Hamed Emami, Ali Mir, and Ali Farmani. *Supersensitive and Tunable Nano-Biosensor for Cancer Detection.* IEEE Sensors Journal 19.13 (2019): 4874-4881. Available: 10.1109/JSEN.2019.2899886

[23] Farmani, Ali, et al. *Highly sensitive nano-scale plasmonic biosensor utilizing Fano resonance metasurface in THz range: numerical study*. Physica E: Low-dimensional Systems and Nanostructures 104 (2018): 233-240. Available: https://doi.org/10.1016/j.physe.2018.07.039

[24] Alipour, Abbas, Ali Farmani, and Ali Mir. *High sensitivity and tunable nanoscale sensor based on plasmon-induced transparency in plasmonic metasurface*. IEEE Sensors Journal 18.17 (2018): 7047-7054. Available: 10.1109/JSEN.2018.2854882

[25] Danaie, Mohammad, and Ali Shahzadi. *Design of a High-Resolution Metal–Insulator–Metal Plasmonic Refractive Index Sensor Based on a Ring-Shaped Si Resonator*. Plasmonics (2019): 1-13.
Available: https://doi.org/10.1007/s11468-019-00926-9

[26] Olyaee, Saeed, et al. *Designing a high sensitivity hexagonal nano-cavity photonic crystal resonator for the purpose of seawater salinity sensing*. Optical and Quantum Electronics 51.4 (2019): 97.
Available: https://doi.org/10.1007/s11082-019-1778-z

[27] Tavakoli, Fatemeh, Ferdows B. Zarrabi, and Hamed Saghaei. *Modeling and analysis of high-sensitivity refractive index sensors based on plasmonic absorbers with Fano response in the near-infrared spectral region*. Applied Optics 58.20 (2019): 5404-5414.
Available: https://doi.org/10.1364/AO.58.005404

[28] Akter, Sanjida, and SM Abdur Razzak. *Highly sensitive open-channels based plasmonic biosensor in visible to near-infrared wavelength*. Results in Physics 13 (2019): 102328.
Available: https://doi.org/10.1016/j.rinp.2019.102328

[29] Xiao, Bo, et al. *Plasmonic pixel biosensor based on grazing angle illumination and computational imaging*. IEEE Sensors Journal (2019). Available: 10.1109/JSEN.2019.2914666

[30] Shukla, Gauri M., et al. *Optimization of Plasmonic U-Shaped Optical Fiber Sensor for Mercury Ions Detection Using Glucose Capped Silver Nanoparticles*. IEEE Sensors Journal 19.9 (2019): 3224-3231. Available: 10.1109/JSEN.2019.2893270

[31] Li, Hongju, et al. "*Investigation of multiband plasmonic metamaterial perfect absorbers based on graphene ribbons by the phase-coupled method*." Carbon 141 (2019): 481-487.
Available: https://doi.org/10.1016/j.carbon.2018.10.002

[32] Keshavarz, Afsaneh, and Zohreh Vafapour. *Sensing avian influenza viruses using Terahertz metamaterial reflector*. IEEE Sensors Journal 19.13 (2019): 5161-5166. Available: 10.1109/JSEN.2019.2903731

[33] Nasirifar, Ruhallah, Mohammad Danaie, and Abbas Dideban. *Dual channel optical fiber refractive index sensor based on surface plasmon resonance*. Optik 186 (2019): 194-204.
Available: https://doi.org/10.1016/j.ijleo.2019.04.104

[34] Shahini, Ali, et al. *Self-powered and transparent all-graphene biosensor*. 2016 IEEE SENSORS. IEEE, 2016.
Available: 10.1109/ICSENS.2016.7808963

[35] Vafapour, Zohreh, et al. *Graphene-based mid-infrared biosensor*. JOSA B 34.12 (2017): 2586-2592.
Available: https://doi.org/10.1364/JOSAB.34.002586

[36] F. Dadoenkova, and F. F. Lee. *Reflection of electromagnetic waves from bigyrotropic negative metamaterials*. Journal of the Korean Physical Society 53.3 (2008). Available: 10.3938/jkps.53.1694

[37] Golmohammadi, Saeed, and Arash Ahmadivand. *Fano resonances in compositional clusters of aluminum nanodisks at the UV spectrum: a route to design efficient and precise biochemical sensors*. Plasmonics 9.6 (2014): 1447-1456. Available: https://doi.org/10.1007/s11468-014-9762-8

[38] Mohammadi, Ghobad, et al. *Chemometrics-assisted investigation of interactions of Tasmar with human serum albumin at a glassy carbon disk: Application to electrochemical biosensing of electro-inactive serum albumin*. Journal of pharmaceutical and biomedical analysis 156 (2018): 23-35. Available: https://doi.org/10.1016/j.jpba.2018.04.021

[39] Rashno, Abdolreza, et al. *Fully automated segmentation of fluid/cyst regions in optical coherence tomography images with diabetic macular edema using neutrosophic sets and graph algorithms*. IEEE Transactions on Biomedical Engineering 65.5 (2017): 989-1001.
Available: 10.1109/TBME.2017.2734058

[40] Zare, Nahid, et al. *Sonochemical synthesis, characterization, biological applications, and DFT study of new nano-sized manganese complex of azomethine derivative of diaminomaleonitrile*. Journal of the Iranian Chemical Society 16.7 (2019): 1501-1516.

Available: https://doi.org/10.1007/s13738-019-01626-1

[41] Raeisi, Moslem, Leila Farahani, and Somaye Shams. "*Effects of chemical fertilizers and biostimulants containing amino acid on yield and growth parameters of broad bean (Viciafaba L.).*" International Journal of Agriculture and Crop Sciences (IJACS) 5.21 (2013): 2618-2621. Available: http://ijagcs.com/.../2618-2621.pdf

[42] Wu, Xiaohu, Ceji Fu, and Zhuomin M. Zhang. *Effect of orientation on the directional and hemispherical emissivity of hyperbolic metamaterials*. International Journal of Heat and Mass Transfer 135 (2019): 1207-1217. Available: https://doi.org/10.1016/j.ijheatmasstransfer.2019.02.066

[43] Wu, Xiaohu, and Ceji Fu. *Ultra-broadband perfect absorption with stacked asymmetric hyperbolic metamaterial slabs*. Nanoscale and Microscale Thermophysical Engineering 22.2 (2018): 114-123. Available: https://doi.org/10.1080/15567265.2018.1434844

[44] Hamzavi-Zarghani, Zahra, et al. *Tunable polarization converter based on graphene metasurfaces*. 2018 IEEE Radio and Antenna Days of the Indian Ocean (RADIO). IEEE, 2018. Available: 10.23919/RADIO.2018.8572341

[45] Hamzavi-Zarghani, Zahra, Alireza Yahaghi, and Ladislau Matekovits. *Reconfigurable metasurface lens based on graphene split ring resonators using Pancharatnam–Berry phase manipulation*. Journal of Electromagnetic Waves and Applications 33.5 (2019): 572-583. Available: https://doi.org/10.1080/09205071.2018.1563509

[46] Patel, Shobhit K., Karan H. Shah, and Y. P. Kosta. *Frequency-reconfigurable and high-gain metamaterial microstrip-radiating structure*. Waves in Random and Complex Media 29.3 (2019): 523-539. Available: https://doi.org/10.1080/17455030.2018.1452309

[47] Dragoman, Daniela, and Mircea Dragoman. *Metamaterials for ballistic electrons*. Journal of applied physics 101.10 (2007): 104316. Available: 10.2528/PIERM10111402

[48] Baqir, Muhammad Abuzar, Aqeel Abbas Syed, and Qaisar Abbas Naqvi. *Electromagnetic fields in a circular waveguide containing chiral nihility metamaterial*. Progress In Electromagnetics Research 16 (2011): 85-93. Available: https://doi.org/10.1063/1.2734876

[49] Ghasemi, Masih, et al. *Metamaterial absorber comprising chromium–gold nanorods-based columnar thin films*. Journal of Nanophotonics 11.4 (2017): 043505. Available: https://doi.org/10.1007/s11082-018-1687-6

[50] Soheilifar, Mohammad Reza. *Wideband optical absorber based on plasmonic metamaterial cross structure.* Optical and Quantum Electronics 50.12 (2018): 442. Available: https://doi.org/10.1117/1.JNP.11.043505

[51] Wang, Tongling, et al. *Tunable polarization-nonsensitive electromagnetically induced transparency in Dirac semimetal metamaterial at terahertz frequencies.* Optical Materials Express 9.4 (2019): 1562-1576. Available: https://doi.org/10.1364/OME.9.001562

[52] Yang, Maosheng, et al. *Electromagnetically induced transparency-like metamaterials for detection of lung cancer cells*. Optics Express 27.14 (2019): 19520-19529. Available: https://doi.org/10.1364/OE.27.019520

[53] Tang, Chao, et al. *Bifunctional resonance effects of classical electromagnetically induced transparency and Fano response using a terahertz metamaterial resonator*. Applied Optics 58.16 (2019): 4414-4419. Available: https://doi.org/10.1364/AO.58.004414

[54] Hajizadegan, Mehdi, Davood Fathi, and Maryam S. Sakhdari. *All-optical metamaterial switch based on Kerr effect with MWCNT composite*. Physica E: Low-dimensional Systems and Nanostructures 48 (2013): 1-6. Available: https://doi.org/10.1016/j.physe.2012.11.001

[55] Estakhri, Nasim Mohammadi, Brian Edwards, and Nader Engheta. *Solving integral equations with optical metamaterial-waveguide networks*. CLEO: QELS_Fundamental Science. Optical Society of America, 2017. Available: https://doi.org/10.1364/CLEO_QELS.2017.FTh1G.2

[56] Khodaee, M., M. Banakermani, and H. Baghban. *GaN-based metamaterial terahertz bandpass filter design: tunability and ultra-broad passband attainment.* Applied optics 54.29 (2015): 8617-8624. Available: https://doi.org/10.1364/AO.54.008617

[57] Ahmadzadeh, Nesa, Zeinab Rashidian, and Abdolrahim Baharvand. *Gate-Controlled Conductance in ABA-Stacked Trilayer Graphene*. Iranian Journal of Science and Technology, Transactions A: Science (2019): 1-7. Available: https://doi.org/10.1007/s40995-019-00716-2

[58] Rashidian, Z., et al. *Valley polarized current and Fano factor in a ferromagnetic/normal/ferromagnetic silicene superlattice junction*. Journal of Magnetism and Magnetic Materials 442 (2017): 15-24. Available: https://doi.org/10.1016/j.jmmm.2017.06.023

[59] Farmani, Ali. *Quantum-dot semiconductor optical amplifier: performance and application for optical logic gates*. Majlesi Journal of Telecommunication Devices 6.3 (2017).

Available: http://journals.iaumajlesi.ac.ir/td/index/index.php/td/article/view/428

[60] Farmani, Ali, Mahmoud Farhang, and Mohammad H. Sheikhi. *High performance polarization-independent Quantum Dot Semiconductor Optical Amplifier with 22 dB fiber to fiber gain using Mode Propagation Tuning without additional polarization controller*. Optics & Laser Technology 93 (2017): 127-132. Available: https://doi.org/10.1016/j.optlastec.2017.02.007

[61] Ann P O'Rourke, and Mariya Lazebnik, *Dielectric properties of human normal, malignant and cirrhotic liver tissue: in vivo and ex vivo measurements from 0.5 to 20 GHz using a precision open-ended coaxial probe*, Phys. Med. Biol. 52 (2007), p.p. 4707–4719. Available: https://doi.org/10.1088/0031-9155/52/15/022

[62] Jichun Li and Yunqing Huang, *Time-Domain Finite Element Methods for Maxwell's Equations in Metamaterials*, ISSN 0179-3632, ISBN 978-3-642-33788-8, 2010, p.p. 8-13. Available: https://infoscience.epfl.ch/record/197899

[63] Rafiee, Esmat, Roozbeh Negahdari, and Farzin Emami. *Plasmonic multi channel filter based on split ring resonators: Application to photothermal therapy*. Photonics and Nanostructures-Fundamentals and Applications 33 (2019): 21-28. Available: https://doi.org/10.1016/j.photonics.2018.11.006

[64] Farmani, Homa, Ali Farmani, and Zeinab Biglari. *A label-free graphene-based nanosensor using surface plasmon resonance for biomaterials detection*. Physica E: Low-dimensional Systems and Nanostructures 116 (2020): 113730. Available: https://doi.org/10.1016/j.physe.2019.113730

[65] Sadeghi, Tannaz, et al. *Improving the performance of nanostructure multifunctional graphene plasmonic logic gates utilizing coupled-mode theory. Applied Physics B 125.10 (2019): 189.* Available: https://doi.org/10.1007/s00340-019-7305-x

[66] Hamzavi-Zarghani, Zahra, et al. *Tunable mantle cloaking utilizing graphene metasurface for terahertz sensing applications. Optics Express 27.24 (2019): 34824-34837.* Available: https://doi.org/10.1364/OE.27.034824

[67] Jabbari, Masoud, et al. *Ultra-Compact Bidirectional Terahertz Switch Based on Resonance in Graphene Ring and Plate*. Journal of Optoelectronical Nanostructures 4.4 (2019): 99-112. Available: http://jopn.miau.ac.ir/article_3761.html

[68] Olyaee, Mohsen, Mohammad Bagher Tavakoli, and Abbas Mokhtari. *Propose, Analysis and Simulation of an All Optical Full Adder Based on Plasmonic Waves using Metal-Insulator-Metal Waveguide Structure*. Journal of Optoelectronical Nanostructures 4.3 (2019): 95-116. Available: http://jopn.miau.ac.ir/article_3622.html

[69] Abdikian, Alireza, GHahraman Solookinejad, and Zahra Safi. *Electrostatics Modes in Mono-Layered Graphene*. Journal of Optoelectronical Nanostructures 1.2 (2016): 1-8. Available: http://jopn.miau.ac.ir/article_2044.html

[70] Servatkhah, Mojtaba, and Hadi Alaei. *The Effect of Antenna Movement and Material Properties on Electromagnetically Induced Transparency in a Two-Dimensional Metamaterials*. Journal of Optoelectronical Nanostructures 1.2 (2016): 31-38. Available: http://jopn.miau.ac.ir/article_2046.html

[71] Izadparast, Ali, and Peyman Sahebsara. *Energy band correction due to one dimension tension in phosphorene*. Journal of Optoelectronical Nanostructures 2.1 (2017): 59-68. Available: http://jopn.miau.ac.ir/article_2201.html

[72] Baroogh Miandoab, Vahid, Esmaiel Saievar Iranizad, and Hemmati Kahrade. *The effect of concentration and time of hydrothermal process on the fluorescent property of Molybdenum Diselenide nano-layers*. Journal of Optoelectronical Nanostructures 1.3 (2016): 35-42. Available: http://jopn.miau.ac.ir/article_2192.html

[73] Jafari, Marjan. *Electronic Transmission Wave Function of Disordered Graphene by Direct Method and Green's Function Method*. Journal of Optoelectronical Nanostructures 1.2 (2016): 57-68. Available: http://jopn.miau.ac.ir/article_2049.html

[74] Rafiee, Esmat, and Farzin Emami. *Design and Analysis of a Novel Hexagonal Shaped Channel Drop Filter Based on Two-Dimensional Photonic Crystals*. Journal of Optoelectronical Nanostructures 1.2 (2016): 39-46. Available: http://jopn.miau.ac.ir/article_2047.html

[75] Alipour, Abbas, Ali Mir, and Ali Farmani. *Ultra high-sensitivity and tunable dual-band perfect absorber as a plasmonic sensor*. Optics & Laser Technology 127 (2020): 106201. Available: https://doi.org/10.1016/j.optlastec.2020.106201

[76] Mozaffari, Mohammad Hazhir, and Ali Farmani. *On-chip single-mode optofluidic microresonator dye laser sensor*. IEEE Sensors Journal (2019). Available: https://doi.org/10.1109/JSEN.2019.2962727

[77] Farmani, Ali, et al. *Optical nanosensors for cancer and virus detections*. Nanosensors for Smart Cities. Elsevier, 2020. 419-432.
Available: https://doi.org/10.1016/B978-0-12-819870-4.00024-4

[78] Farmani, Ali, and Ali Mir. *Nanosensors for street-lighting system*. Nanosensors for Smart Cities. Elsevier, 2020. 209-225.
Available: https://doi.org/10.1016/B978-0-12-819870-4.00012-8

[79] Ghodrati, Maryam, Ali Mir, and Ali Farmani. *Carbon nanotube field effect transistors–based gas sensors*. Nanosensors for Smart Cities. Elsevier, 2020. 171-183.
Available: https://doi.org/10.1016/B978-0-12-819870-4.00036-0